03,16,10

Random laser generation in ZnO nanocrystals grown by hydrothermal method

© M.E. Labzovskaya[1], B.V. Novikov[1], A.Yu. Serov[1], S.V. Mikushev[1], S.A. Kadinskaya[2,3], V.M. Kondratiev[2,3], A.D. Bolshakov[2,3], A.I. Likhachev[4], A.V. Naschekin[4], Yu.B. Samosenko[2,5], I.V. Shtrom[1,5]

[1] St. Petersburg State University,
St. Petersburg, Russia
[2] Alferov Academic University, RAS,
St. Petersburg, Russia
[3] Moscow Institute of Physics and Technology (State University),
Dolgoprudnyi, Moscow oblast, Russia
[4] Ioffe Institute,
St. Petersburg, Russia
[5] Institute of Analytical Instrument Making, Russian Academy of Sciences,
St. Petersburg, Russia

E-mail: xrul@mail.ru

Received October 20, 2023
Revised October 20, 2023
Accepted October 21, 2023

The possibility of laser generation was found in nanocrystalline ZnO samples of various morphologies grown using the hydrothermal growth method. It is shown that at a high optical excitation density, the arrays of ZnO nanowires forming the surface of the samples are self-organizing systems demonstrating random laser radiation generation with a relatively low excitation threshold. The relationship between the generation occurrence and the morphology of nanocrystals has been established. Possible generation mechanisms are discussed.

Keywords: zinc oxide, hydrothermal synthesis, nanowhiskers, random laser generation.

DOI: 10.61011/PSS.2024.01.57847.235

1. Introduction

Semiconductors with a wide band gap have been of much interest for a long time due to the prospects of application in light-emitting devices. Among a few candidates, zinc oxide features technological availability and high chemical stability. Modern methods are used to produce ZnO-based high-quality nanocrystalline structures using relatively simple and cheap techniques and the electronic properties of ZnO — wide band gap (3.37 eV at room temperature) and high exciton bond energy (60 meV), make ZnO-based structures very attractive for the use as effective laser material and in opto-electronic instruments designed for operation at room temperature [1–3]. Manufacturing of ZnO films, quantum wells, nanowires and nanocrystals have been always a promising area, including in terms of achievement of effective laser medium.

Laser generation in ZnO has been earlier investigated in [4–6]. In particular, our group has a set of publications on the topic [7–9]. Laser generation in disordered systems is of special interest. Bolshakov's group has demonstrated hydrothermal growth of ZnO nanocrystals that ensured morphology control of synthesized structures [10]. This study investigates whether laser generation may be achieved when using ZnO nanocrystal arrays with different morphology. The study also addresses possible generation mechanisms.

2. Samples and experimental technique

Photoluminescence was studied using „Janis Research Company" closed-cycle helium cryostat in the temperature range of 5−300 K. MDR-204-2 (LOMO-Photonics, St. Petersburg) double monochromator with a dispersion of 25 A/mm was used. PL spectra were excited by He−Cd laser ($\lambda = 325$ nm, $W = 10$ mW) and LCM-DTL-374QT ($\lambda = 355$ nm) ultraviolet solid-state laser. Emission power of the latter varied in the range from 1 to 800 kW/cm^2. Direct-geometry study was conducted. The samples were irradiated and, accordingly, the signal was recorded either in the sample plane or end, normally on a side face.

We have earlier studied in detail series of ZnO samples grown by the hydrothermal method on silicon substrate [10]. It has been shown that growth conditions have a fundamental influence on the morphological and related optical properties of zinc oxide nanocrystals. The study identified two main types of samples.

Group A. All samples of this group were nanowhiskers with various orientation on the substrate surface. In some cases, whiskers formed visually random or structures clusters and were rod-shaped with length-thickness ratio of about 10 : 1 (Figure 1). In low-temperature PL spectra Group A samples with PLA excitation by a relatively low-power He−Cd laser, an emission band of exciton D_0X localized on a neutral donor (a narrow

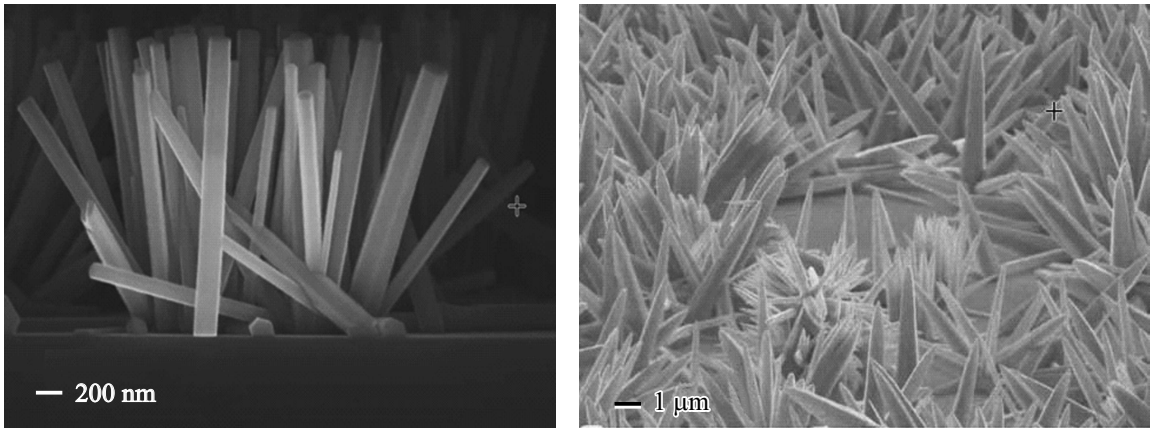

Figure 1. SEM images of sample surface, Group A.

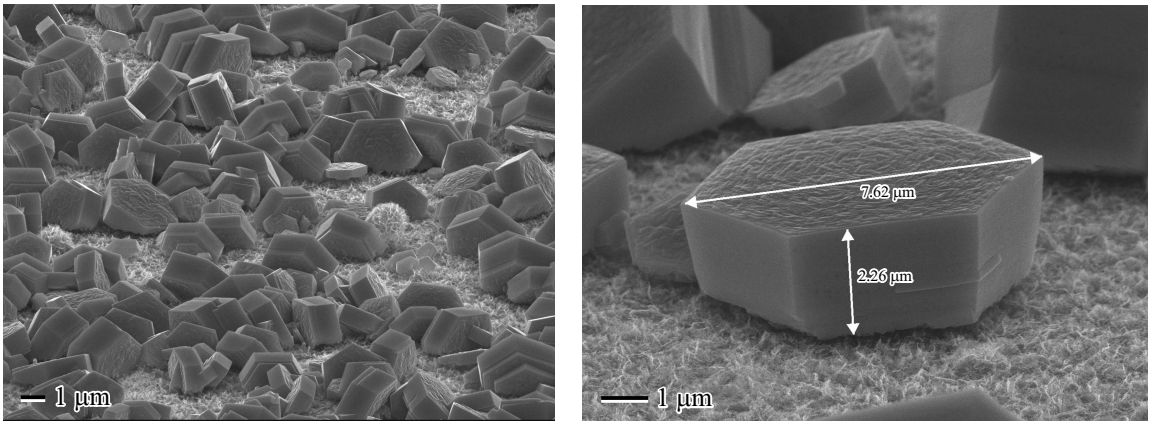

Figure 2. SEM images of sample surface, Group B.

band with peak $\lambda = 369.1$ nm) and emission attributed to the electron–acceptor eA transition (broad band at $\lambda = 375.5$ nm) were usually present. It should be noted that this spectral band also includes P — emission band of the exciton–exciton interaction ($\lambda = 374.4$ nm) that occurs at high excitation density [11].

On the other hand, the samples **Group B** were assemblies of regular hexagon-shaped microcrystals $\sim 7\,\mu$m in diameter and $\sim 2{-}3\,\mu$m in height (Figure 2). Only one intense line D_0X was observed in the emission of this sample group.

3. Findings and discussion

PL behavior of both types of the above ZnO samples was investigated herein with excitation laser power variation. It has been found that whisker arrays, primarily of Group A samples, at high excitation density constituted some self-organized systems exhibiting random emission generation with a relatively low excitation threshold. The emission pattern varied according to the chosen region on the sample surface, but remained similar in its main spectral characteristics. Figure 3 shows the photoluminescence spectra evolution in one of the selected points on Group A ZnO sample with an increase in the excitation laser power measured when the sample surface was exposed to emission at $T = 5$ K. As shown in the figure, at low excitation levels (Detail in Figure 3, curve *8*) the PL spectra demonstrate an emission pattern that is typical for this type of samples and described above — a bound exciton line ($\lambda = 369$ nm) and electron — acceptor band ($\lambda = 375$ nm) [12,13]. The spectrum shape varies with increasing excitation power — a long-wave band is getting more intense (curves *1–7*), quickly becomes dominating in the spectrum and transforms into an intense narrow peak that moves towards the long-wavelength region from $\lambda = 374.5$ to 376.2 nm (see Figure 3). In the short-wavelength region of the spectrum, however, an emission arm probably belonging to P band is still observed.

Figure 4 shows the emission behavior for another region of the same sample. It is apparent that at high pumping levels PL spectrum of this point contains not one, as in Figure 3, but three narrow emission peaks in the spectral region $\lambda < 375$ nm. Apart from that, the emission variation behavior and spectral characteristics of two points almost

coincide. Detail in Figure 4 shows the integrated luminescence variation with increasing optical pumping. Kinking of the approximating straight lines shows the induced emission threshold. With approximation of the experimental points by straight lines, the kink falls on $W < 95\,\text{kW/cm}^2$. Thus, $95\,\text{kW/cm}^2$ is suggested to be the generation threshold in these samples.

Similar investigations were carried out for Group B samples. Figure 5 shows the PL spectra variation with growing intensity of the excitation laser for a sample of this group. It has been found that the PL spectrum at low

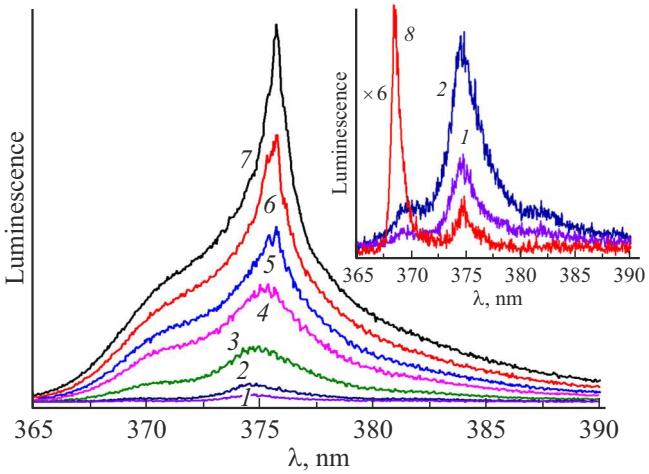

Figure 3. Photoluminescence spectra of ZnO nanowhiskers, Group A, with increasing pumping power W. $T = 5\,\text{K}$. **Point 1.** *7* — $W = 753$, *6* — 570, *5* — 440, *4* — 344, *3* — 177, *2* — 77, *1* — $36\,\text{kW/cm}^2$; Curve *8* — sample PL with low excitation by He–Cd-laser ($\lambda = 325\,\text{nm}$, $W = 10\,\text{mW}$).

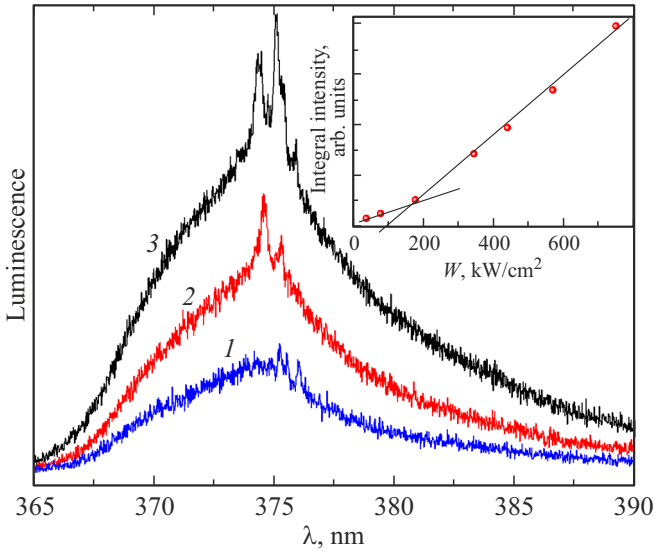

Figure 4. photoluminescence spectra of ZnO nanowhiskers, Group A, with increasing pumping power W. $T = 5\,\text{K}$. **Point 2.** *1* — $W = 210$, *2* — 390, *3* — $620\,\text{kW/cm}^2$. Detail: integrated luminescence variation with increasing excitation laser power W.

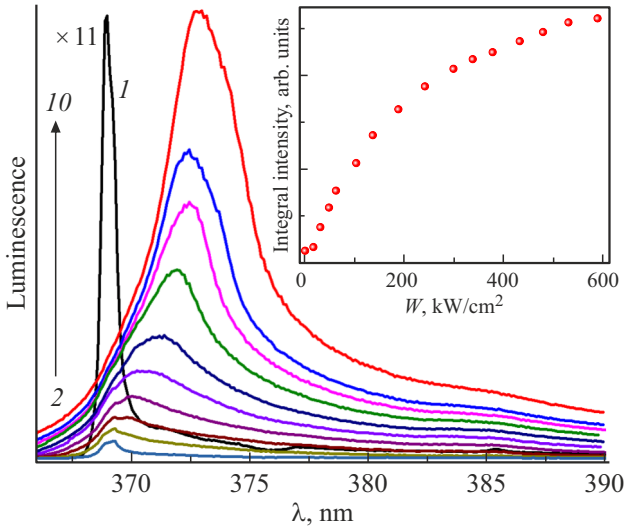

Figure 5. Photoluminescence spectra of ZnO nanowhiskers, Group B, with increasing pumping power. $T = 5\,\text{K}$. Curves *2–10* are arranged in the order of increasing of the excitation laser intensity from 0.6 to $600\,\text{kW/cm}^2$. Curve *1* — sample PL with low excitation by He–Cd-laser ($\lambda = 325\,\text{nm}$, $W = 10\,\text{mW}$). Detail: integrated luminescence variation with increasing excitation laser power W.

excitation intensity as described above contains only donor-bound exciton emission $\lambda \cong 369.1\,\text{nm}$ (Figure 5, curve *1*). With higher pumping, the emission spectrum is transformed and a broad band occurs in the 370 nm. spectral range. With further increase in excitation, this band becomes more intense, broader and moves towards the long-wavelength range up to $\lambda = 372.5\,\text{nm}$. Variation of the integrated luminescence with increasing excitation laser power W as shown in Figure 5 demonstrates the PL intensity saturation tendency with growing W. The emission spectrum remain smooth, no induced emission peaks are observed in any of the investigated points on the sample surface.

PL pattern of this sample, however, varies with experiment geometry variation. In case of luminescence excitation and, accordingly, recording at the end normal to the sample side face, the PL spectra contain narrow peaks at $\lambda \cong 372–376\,\text{nm}$ (Figure 6). It is apparent that more ZnO nanocrystals participate in the emission in this case, which allows self-organizing systems to be formed as described for Group A samples.

Summing up all aforesaid, a conclusion can be made that a random laser generation model is implemented on the self-organizing systems consisting of ZnO nanocrystals arranged on the sample substrate in a chaotic or structured manner.

It is obvious that the accumulation and mutual arrangement of whiskers enable formation of closed loops that serve as a resonant cavity for emission generation. Multiple passes of the induced emission over the closed loop apparently form a standing wave which, in turn, results in the occurrence of narrow peaks (modes) in the emission

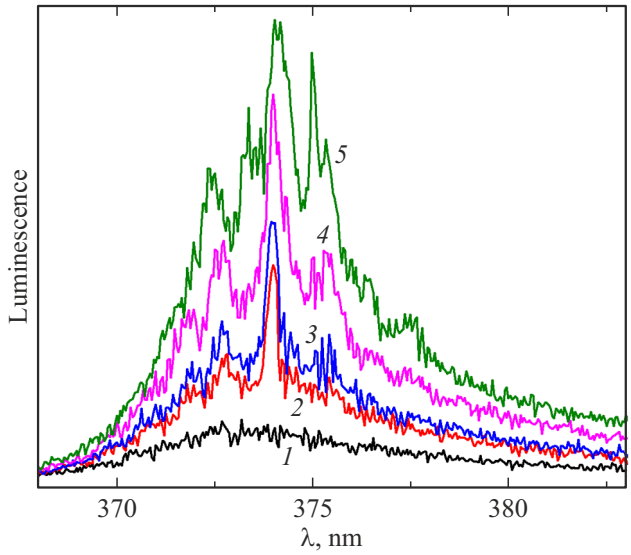

Figure 6. Photoluminescence spectra of ZnO sample, Group B, with increasing pumping power in the sample end geometry.$T = 5$ K. *1* — $W = 130$, *2* — 264, *3* — 408, *4* — 509, *5* — 535 kW/cm^2.

spectra. In our previous papers [8,9], such effect was observed in ZnO produced by laser-induced breakdown of Zn metal in oxygen. Self-organized tube-like nanoparticles demonstrated the random laser generation capability at room temperature. The induced emission mechanism in the maximum gain region was described in these papers as the exciton recombination with emission of two LO phonons.

Laser generation in ZnO nano- and microcrystals prepared by hydrothermal method was investigated. Dependence of laser generation processes on the sample morphology was detected. It is shown that laser generation is observed in most points on Group A samples. nanowhiskers in such samples are arranged on the surface either chaotically or with a slight inclination to the substrate surface. In Group B samples (hexagon microcrystals), laser generation depends on the excitation and observation geometry [5,6]. In this and the other case, random laser generation is referred to. Thin lines on the smooth emission outline correspond to closed loops of resonant cavities where laser generation conditions occur. Spectral position of these lines indicates that laser generation most likely occurs near P band of the exciton–exciton interaction [14].

Acknowledgments

S.A. Kadinskaya would like to express gratitude to the Ministry of Science and Higher Education of the Russian Federation (grant No. FSRM-2023-0009) for nanostructure synthesis support. V.M. Kondratiev would like to express gratitude to the Ministry of Science and Higher Education (Agreement 075-03-2023-106 as of 13.01.2023, Project FSMG-2021-0005) for SEM characterization support.

Funding

The optical research was supported financially by grant of St. Petersburg State University No. 94033852.

Conflict of interest

The authors declare that they have no conflict of interest.

References

[1] D.C. Look, B. Claflin, Y.I. Alivov, S.J. Park. Phys. Status Solidi **201**, 2203 (2004).
[2] S. Chu, G. Wang, W. Zhou, Y. Lin, L. Chernyak, J. Zhao, J. Kong, L. Li, J. Ren, J. Liu. J. Nature Nanotechnol. **6**, 506 (2011).
[3] J.H. Na, M. Kitamura, M. Arita, Y. Arakawa. Appl. Phys. Lett. **95**, 253303 (2009).
[4] Ü. Özgür, Ya.I. Alivov, C. Liu, A. Teke, M.A. Reshchikov, S. Doan, V. Avrutin, S.-J. Cho, H. Morkoç. J. Appl. Phys. **98**, 04130 (2005).
[5] S.F. Yu, Clement Yuen, S.P. Lau, W.I. Park, Gyu-Chul Yi. Appl. Phys. Lett. **84**, 3241 (2004).
[6] A.N. Gruzintsev, A.N. Redkin, Z.I. Makovey, E.E. Yakimov, C. Barthou. FTP **41**, *6*, 730 (2007). (in Russian).
[7] I.Kh. Akopyan, B.V. Novikov, A.Yu. Serov. FTT **63**, *12*, 2157 (2021). (in Russian).
[8] N. Vasilyev, E.N. Borisov, B.V. Novikov, I.Kh. Akopyan. J. Luminescence **215**, 116668 (2019).
[9] Nikolay Vasilyev, B.V. Novikov, I.Kh. Akopyan, M.E. Labzovskaya. J. Luminescence **182**, 45 (2017).
[10] S. Kadinskaya, V. Kondratev, I. Kindyushov, O. Koval, D. Yakubovsky, A. Kusnetsov, A. Lihachev, A. Nashchekin, A. Serov, S. Mikushev, B. Novikov, I. Shtrom, A. Bolshakov. Nanomaterials **13**, *1*, 58 (2023).
[11] D.M. Bagnall, Y.F. Chen, Z. Zhu, T. Yao. Appl. Phys. Lett. **73**, 8 (1998).
[12] I.Kh. Akopyan, B.V. Novikov, A.Yu. Serov, N.G. Filosofov, N.R. Grigor'eva. FTT **62**, *11*, 1902 (2020). (in Russian).
[13] I.Kh. Akopyan, B.V. Novikov, A.Yu. Serov. FTT **63**, *12*, 2157 (2021). (in Russian).
[14] C. Klingshirn, J. Fallert, H. Zhou, J. Sartor, C. Thiele, F. Maier-Flaig, D. Schneider, H. Kalt. Phys. Status Solidi B **6**, 1424 (2010).

Translated by E.Ilinskaya